International Journal of Thermophysics, Vol. 15, No. 5, 1994

Quasi-Isochoric $p\rho T$ Measurements and Second Virial Coefficient of *n*-Heptane

J. Millat,[1,2] H. Hendl,[3] and E. Bich[3]

Received June 8, 1994

Quasi-isochoric $p\rho T$ measurements on *n*-heptane vapor were carried out in the low density region using an improved apparatus that was originally proposed by Opel and Schaffenger (*Wiss. Z. Univ. Rostock* **N18**:871, 1969). The experimental results extend over the temperature range between 350 and 600 K and the density range between 11.5 and 52.2 mol · m^{-3}. Above 473 K a small but significant influence of decomposition was found. Accordingly, a correction scheme assuming a trace of decomposition products was applied to these data. Second virial coefficients were derived with an assumed maximum uncertainty of ±3%. The results are compared with others in the literature and used to develop an improved correlation function for the temperature dependence of $B(T)$.

KEY WORDS: correlation; *n*-alkanes; $p\rho T$ measurements; second virial coefficient.

1. INTRODUCTION

Starting with the pioneering work of van der Waals, Clausius, Kamerlingh Onnes, and others, the analysis of the $p\rho T$ surface of fluids has been of interest for many scientists. This is true for experimental as well as theoretical work and due to the fact that the results of those studies are of great importance for practical purposes *and* in the field of basic science.

Recent interest in emerging technologies, including petrochemistry and methanol-based chemistry, has led to an increasing need for physical property data of aromatic compounds, *n*-alkanes, alkanols, water, and mixtures of these species.

[1] NORDUM GmbH, Gewerbepark Am Weidenbruch, D-18196 Kessin/Rostock, Germany.
[2] To whom correspondence should be addressed.
[3] Universität Rostock, Fachbereich Chemie, D-18051 Rostock, Germany.

0195-928X/94/0900-0903$07.00/0

These situation forms the background of the work of the IUPAC Subcommittee on Thermodynamic Data on "Vapor-Liquid Equilibria in Alkan-1-ol + *n*-Alkane Mixtures." Since the volumetric properties of pure components are always essential in this context, the given need for data also formed the basis for studies on the $p\rho T$ behavior of benzene [1] and *n*-alkanes [2, 3] which were started in this laboratory some years ago.

Dymond et al. [4] published an analysis concerning second virial coefficients for C_1–C_8 alkanes in 1968. It became obvious from this study that the uncertainty of correlated data is increasing with increasing carbon number. A subsequent paper by Tsonopoulos et al. [5] led to an improvement for the representation of the second virial coefficient of *n*-butane, *n*-pentane, and *n*-hexane. But no data for higher *n*-alkanes could be included.

Therefore, a study of the low-density $p\rho T$ behavior of *n*-heptane was carried out using a quasi-isochoric method that was originally applied by Opel and Schaffenger [1, 2, 6]. Here, results of these measurements in the temperature range from 375 to 600 K and in the density range between 11.5 and 52.2 $\text{mol} \cdot \text{m}^{-3}$ are presented.

From a preliminary analysis it became obvious that there was a small, but significant influence of decomposition above 473 K. Since the amount of decomposition products can be assumed to be small, the $p\rho T$ data could be corrected for this effect.

These corrected data together with those for temperatures below 473 K enabled second virial coefficients to be evaluated. The latter were used together with data from the literature to derive an improved correlation for $B(T)$ in the temperature range $350 \leqslant T \leqslant 600$ K.

2. EXPERIMENTS

2.1. Apparatus

During the sixties and seventies, Opel and co-workers studied the low-density behavior of organic vapors, water, and mixtures of such substances using a quasi-isochoric method (for a survey cf. Ref. 7). The general design of this apparatus is given in Fig. 1. The main part consists of a two-chamber (A, B) constant volume cell (1) completely made of quartz. The measuring chamber (A) is including a quartz-spoon zero-pressure indicator (2). The temperature is measured applying a platinum-resistance thermometer (4) placed in the thermometer housing almost in the center of chamber A. The cell is placed in a high-temperature air-bath thermostat consisting of an electronically controlled aluminium-alloy furnace (7). To

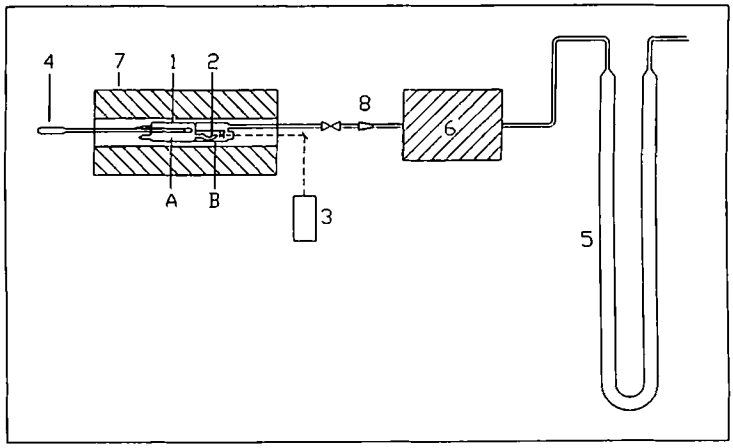

Fig. 1. Schematic diagram of the experimental setup: (1) quartz cell, (A) measuring chamber and (B) reference chamber; (2) quartz-spoon gauge; (3) optical device; (4) platimum-resistance thermometer; (5) mercury U-tube manometer; (6) reference pressure control unit; (7) thermostat; (8) fitting.

avoid or at least reduce decomposition, the quartz-spoon gauge (2) is used as a pressure transducer between A and the reference chamber B. Its zero position was observed using a special optical system (3). The reference part (B + 6) is filled with argon or nitrogen and connected to the mercury U-tube manometer (5) that is applied to measure the pressure. From our experience the quartz cell could be used up to pressures of 0.4 MPa provided the pressure difference between the two parts A and B is kept as small as possible. Nevertheless, the range of our measurements was restricted to maximum pressures of 0.26 MPa because of the dimensions of the U-tube manometer.

Although the general design of the apparatus described in Ref. 6 remained unchanged, numerous details were improved [8]. Furthermore, several correction schemes to be applied to weighing, pressure, and volume measurements were checked and improved if possible [8]. Since the $p\rho T$ behavior of permanent gases cannot be analyzed with this apparatus, vapor pressure, and $p\rho T$ measurements of benzene served as a performance test [1, 8].

2.2. Substance

n-Heptane ("highly pure for gas chromatography") with a stated content of 99.942% was supplied by PCK Schwedt AG and was used

without further purification. The liquid was dried with molecular sieves 4A. After five rounds of high-vacuum sublimation, the degassed substance was filled into small glass ampoules. The samples were characterized by gas chromatographic analysis (Hewlett-Packard 5880A gas chromatograph, 50-m capillary, OV-1, 30°C, FID). According to this analysis the final purity of the substance was 99.952%.

2.3. Measurements and Accuracy

The principle of the applied method is to analyze the low-density $p\rho T$ behavior of vapors measuring the four thermodynamic quantities pressure (p), volume (V), mass (m), and temperature (T).

The mass was found by weighing before and after filling the ampoules. Following several corrections, the maximum uncertainty associated to this quantity was found to be ± 6 μg. The cell volume at room temperature (V_0) was determined by weighing it with three times distilled and degassed water and applying the needed corrections such as buoyancy correction, etc., to the results of weighing as well. For this study two cells were used, with $V_0 \approx 153\ \text{cm}^3$ and $V_0 \approx 145\ \text{cm}^3$, respectively (see Table I). Above room temperature the volume was corrected for thermal expansion of the quartz glass. The maximum uncertainty associated to the determination of V was assumed to be $\pm 0.016\ \text{cm}^3$.

Mass m, molar mass M, and volume V were used to calculate the molar density ρ with a maximum uncertainty of $\pm 0.006\ \text{mol} \cdot \text{m}^{-3}$. The temperature was measured with a maximum uncertainty of $\pm 0.005\%$ (± 0.03 K at 600 K).

Table I. Range of Thermodynamic States Analyzed in this Study

Series	Amount of substance (10^{-3} mol)	Volume at room temp. (cm^3)	Mean density ($\text{mol} \cdot \text{m}^{-3}$)	Temperature range (K)	Pressure range (kPa)	Number of points
H7-6	1.67460	145.10	15.18	374–598	33–57	33
H7-8	2.36543	145.59	16.24	374–598	45–80	33
H7-1	3.20126	153.45	20.86	374–598	63–103	33
H7-4	3.83592	153.37	25.01	374–598	75–123	30
H7-10	4.54598	145.54	31.23	374–598	92–154	30
H7-2	5.09324	153.67	33.14	397–598	98-163	37
H7-7	5.91341	153.41	38.54	396–599	121–188	30
H7-3	6.56618	152.91	42.94	397–599	134–210	33
H7-9	7.32574	153.15	47.83	397–599	148–233	27
H7-5	7.99216	153.08	52.20	397–598	161–254	27

The maximum uncertainty of the pressure readings was assumed to be ± 15 Pa; the reproducibility was found to be even better.

In order to measure one isochore the following steps were necessary: Before loading the samples, the cell was placed in the thermostat (7) and the zero position of the quartz-spoon gauge was determined as a function of temperature at atmospheric pressure. In the next step chambers A and B were evacuated at about 650 K. The vacuum had to be better than 5×10^{-3} Pa for a minimum of 3 h. Then the special thermostat was switched off. The ampoule was loaded at room temperature using a special magnetic device and chamber A was closed by the glassblower. Next, the reference chamber B was carefully filled with argon or nitrogen up to about the vapor pressure of *n*-heptane at ambient temperature. This was necessary in order to reduce the danger of destroying the quartz spoon when the sample was broken in the following step. The cell was then placed in the thermostat (7) and connected to the reference part (6). The actual measurements started with the determination of the sensitivity of the quartz spoon. For this study this was found to be 3–4 Pa per scale unit and independent of temperature within the experimental uncertainty. The isochore was analyzed starting with the lowest temperature. About 45–60 min was needed in order to reach equilibrium. After that, first the temperature was measured, then the position of the quartz-spoon gauge, was recorded, the pressure was determined using the U-tube manometer, and finally, the temperature was measured again. This procedure was repeated at least two times for each temperature.

Following the completed run, the temperature was reduced to ambient temperature. The cell was removed from the thermostat and opened carefully. It was evacuated applying the same conditions as mentioned above for the cell preparation. Finally, the volume of chamber A was determined as described before.

3. RESULTS

Ten isochores in the low-density region were measured. General information about these data is provided in Table I; the $p\rho T$ data (corrected as detailed in Sections 4.1 and 4.2) are given in the Appendix (Table AI). To be able to compare the results to data from the literature, a survey of available data was carried out. This is schematically summarized in Fig. 2. It becomes evident from this graph that only a few data overlap with the range of thermodynamic states that was analyzed in this study. On the other hand, the data measured are especially useful to derive second virial coefficients because the low-density range was chosen. These can be compared to data presented in the studies mentioned before (e.g., Ref. 4).

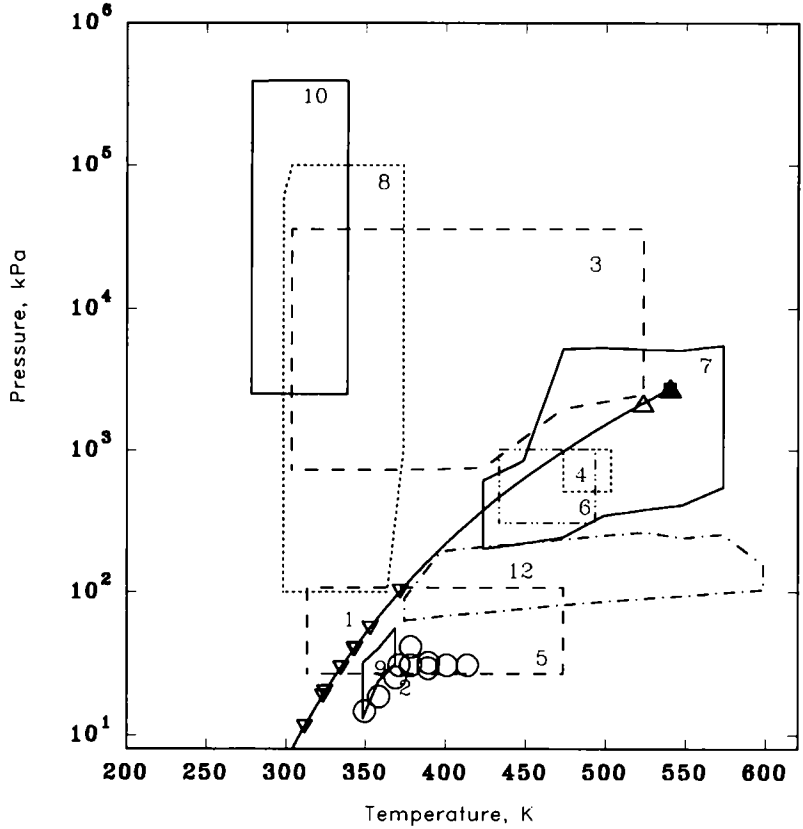

Fig. 2. Survey of experimental $p\rho T$ information. (1) ▽ [24]; (2) ○ [13], △ [27]; (3) ---- [17]; (4) ····· [20]; (5) ---- [14]; (6) -.-.-.- [15]; (7) —— [22]; (8) ····· [25]; (9) —— [16]; (10) —— [26]; (11) ------ [21]; (12) -.-.- this work.

4. DISCUSSION

4.1. Correction for Nominal Temperatures

Although an improved electronical temperature control unit was used, the air bath thermostat was not sufficient to reproduce the temperatures for selected isotherms *exactly*. On the other hand, it is always advisable to analyze isotherms with respect to a physically reasonable behavior first.

Since the differences between nominal (T_{nom}) and experimental (T_{exp}) temperatures were found to be small, the following correction scheme could be applied: According to the virial equation of state

$$p = \rho RT(1 + B\rho + C\rho^2 + \cdots) \tag{1}$$

the derivative $(\partial p/\partial T)_\rho$ in the expression

$$p(T_{nom}) = p(T_{exp}) + \left(\frac{\partial p}{\partial T}\right)_\rho \Delta T + R_n \tag{2}$$

equals

$$\left(\frac{\partial p}{\partial T}\right)_\rho = \frac{p}{T_{exp}} + \rho R T_{exp}\left[\rho\frac{\partial B}{\partial T} + \rho^2\frac{\partial C}{\partial T} + \cdots\right] \tag{3}$$

Here $\Delta T = T_{nom} - T_{exp}$ and R_n is the residual that is given by

$$R_n = \frac{\Delta T^2}{2}\left(\frac{\partial^2 p}{\partial T^2}\right)_\rho (T_{exp} + \vartheta\Delta T) \tag{4}$$

where $0 < \vartheta < 1$. Furthermore, in a first approximation $C(T) = 0$ can be assumed because the measurements were carried out in the low-density region. This leads to

$$p(T_{nom}) = p(T_{exp}) + \left[\frac{p}{T_{exp}} + \rho^2 R T_{exp}\frac{\partial B}{\partial T}\right]\Delta T \tag{5}$$

where $B(T)$ and, therefore, $\partial B/\partial T$ in a first step were taken from the literature [4].

The residual was found to be $R_n \leqslant 0.28$ Pa in all cases and, therefore, much smaller than the experimental uncertainty (15 Pa). Accordingly, Eq. (5) was found to be sufficient within the given range of thermodynamic states.

The resulting isotherms are presented in Fig. 3. From this graph it becomes obvious that the behavior above 473 K is physically not reasonable because it would lead to increasingly negative third virial (remainder) coefficients with increasing temperature, whereas model calculations and numerous experimental results for other substances in the same reduced temperature range lead to positive values.

Following the experience reported in Refs. 3 and 9, it was, therefore, assumed that the given result is due to a small, but significant influence of decomposition at higher temperatures.

The anomalous behavior of the data at 373 K may be due to adsorption. But the even more restricted density range at this temperature was not sufficient for a detailed analysis.

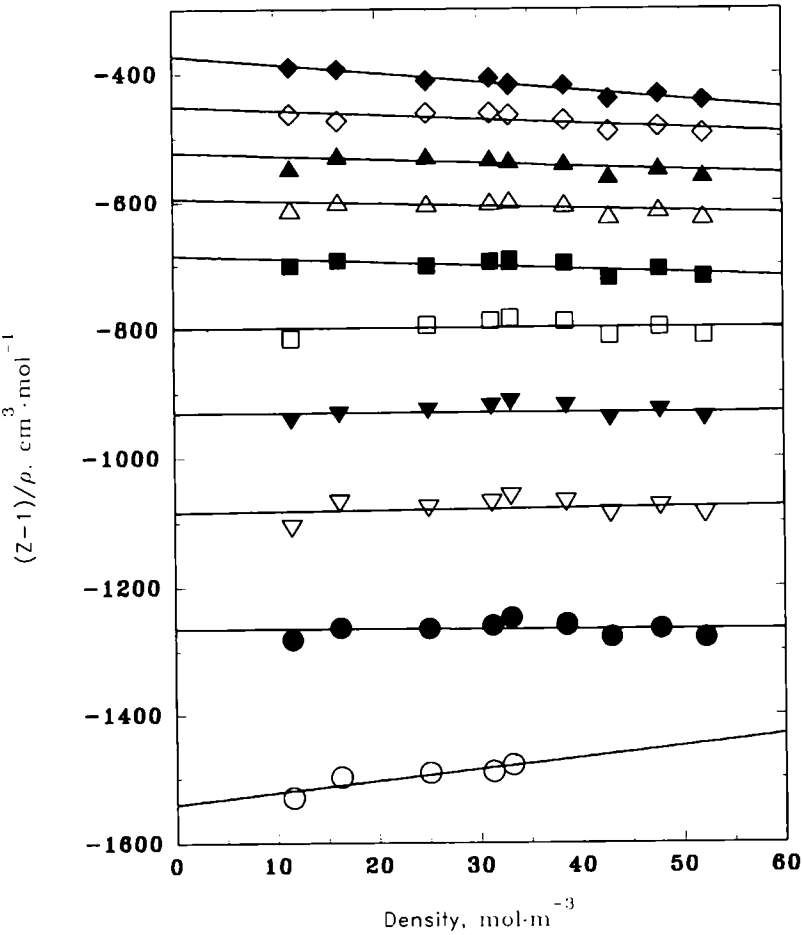

Fig. 3. Isotherms corrected for nominal temperatures: (○) 373.78 K; (●) 396.85 K; (▽) 421.65 K; (▽) 446.12 K; (□) 473.17 K; (■) 496.13 K; (△) 524.64 K; (▽) 5547.64 K; (○) 573.39 K; (◆) 598.40 K.

4.2. Correction for Decomposition

Decomposition always means an increased number of particles, and accordingly the "substance" becomes a mixture with a trace of decomposition products. Since the number of additional particles can be assumed to be small, the following scheme was applied to the raw data for measurements above 473 K:

For a mixture consisting of the main component and a trace of decomposition products, we can roughly assume that

$$\frac{p}{RT} = \rho[1 + \rho(x_1^2 B_{11} + 2x_1 x_2 B_{12} + x_2^2 B_{22})] \tag{6}$$

Here, we again introduce the approximation that the contribution of third virial coefficients is negligible. For the trace then holds

$$x_2 \to 0. \qquad \text{This leads to} \qquad x_1 \to 1 \tag{7}$$

and

$$Z = \frac{p}{\rho RT} = [1 + \rho x_1^2 B_{11}] = a_1 + a_2 \rho \tag{8}$$

The ideal gas behavior in the limit of zero density would require

$$a_1 = 1 \tag{9}$$

In this case one would find

$$a_2 = B_{11} \tag{10}$$

On the contrary, we have in the case of decomposition

$$a_1 \neq 1 \tag{11}$$

To correct for this effect, we have to introduce

$$\rho' \to a_1 \rho \tag{12}$$

Accordingly, the corrected compression factor is

$$Z' = \frac{p}{\rho' RT} = b_1 + b_2 \rho' + \cdots \tag{13}$$

This can be related to the second virial coefficient. Correction factors a_1 as introduced in Eqs. (11) and (12) are detailed in Table II.

Table II. Correction factors a_1 in Eq. (12)

	Temperature (K)					
	473.17	496.13	524.13	547.64	573.39	598.40
a_1	1.00034	1.00056	1.00051	1.00066	1.00074	1.00110

It is worth noting here that a similar anomalous behavior that can be the result of decomposition was also found for *n*-hexane ($T > 574$ K) [2], *n*-octane ($T > 443$ K) [3], and even benzene ($T > 574$ K) [1]. Since this has been analyzed in detail only for *n*-octane up to now, a reanalysis of the data presented in Refs. 1 and 2 may be advisable, although the effect will be small.

4.3. Evaluation of Second Virial Coefficients

The virial equation of state truncated after the third term, i.e.,

$$Z = \frac{p}{\rho RT} = 1 + B(T)\,\rho + C(T)\,\rho^2 \tag{14}$$

was used together with the corrected $p\rho T$ data to evaluate the second virial coefficient. (Here ρ is the "true" density now, i.e., $\rho = \rho'$ above 473 K.)

Different schemes for the evaluation of second virial coefficients have been checked (cf. Refs. 1–3). First, we assumed negligible third virial coefficients. This enabled second virial coefficients to be evaluated directly from each $p\rho T$ set:

$$B(T) = \frac{Z-1}{\rho} = \frac{(p/\rho RT)-1}{\rho} \tag{15}$$

Equation (15) leads only to a rough approximation of $B(T)$ because of the sometimes strong influence of random errors. Therefore, the results of these calculations were used only as a first check for systematic errors in the raw data and are not included in Table III.

Table III. Second Virial Coefficients Derived Using Different Evaluation Schemes

Temperature (K)	$B(T)$ ($cm^3 \cdot mol^{-1}$) isotherms [Eq. (14)]		$B(T)$ ($cm^3 \cdot mol^{-1}$) surface fit		$C(T)$ ($cm^6 \cdot mol^{-2}$)
	$C(T) = 0$ (set 1)	$C(T) \neq 0$ (set 2)	$C = 0$ (set 3)	$C(T) \neq 0$ [11] (set 4)	[11]
396.85	−1267.	−1259.	−1269.	−1269.	15,321
421.65	−1080.	−1082.	−1081.	−1085.	101,458
446.12	−930.3	−927.0	−935.1	−940.6	132,426
473.17	−810.7	−827.6	−807.3	−813.2	139,252
496.13	−724.1	−732.1	−718.7	−724.4	135,221
524.64	−628.3	−638.9	−627.4	−632.6	125,402
547.64	−566.2	−577.8	−565.1	−569.8	116,302
573.39	−501.7	−514.4	−504.5	−508.9	106,218
598.40	−457.9	−467.8	−453.0	−457.1	97,072

It is more sensible to derive virial coefficients from a fit of isotherms to the virial equation of state [e.g., Eq. (14)]. To this end, we used the isotherms derived as discussed in Section 4.1 including the correction for decomposition above 473 K. They were analyzed assuming first that $C(T)=0$ (set 1 in Table III). Next it was assumed that $C(T)\neq 0$ and the complete Eq. (14) was applied (set 2). The results indicated that the $p\rho T$ data presented here lead to small third virial remainder coefficients [10] (see Fig. 4). Furthermore, the conclusion could be drawn that all but the 374 K isotherm (which was excluded from the following analysis) show a physically reasonable behavior now. However, the density range analyzed

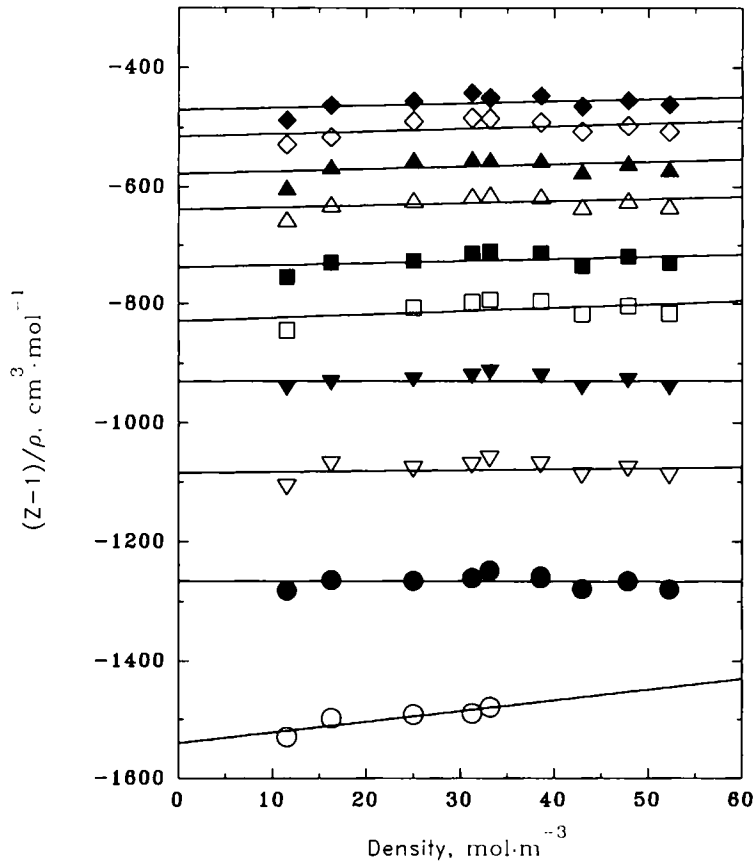

Fig. 4. Isotherms at nominal temperatures, but corrected for decomposition for $T>473$ K (symbols as in Fig. 3); lines from Eq. (14).

turned out to be not sufficient to derive "true" third virial coefficients, therefore, these numbers are not detailed here.

Finally, a surface fit can be carried out. Again, it can be assumed that $C(T)=0$ (*a*). On the other hand, the results derived from single isothermes indicated that $C(T)\neq 0$. This means that the data should be analyzed (b) including a fixed $C(T)$ function (for instance, the Orbey and Vera scheme [11]; see Table III) or (c) using the $p\rho T$ data in order to determine $B(T)$ and $C(T)$ simultaneously. The latter scheme evidently requires a sufficient density range that was not given for the measurements presented. Therefore, only schemes a and b were used.

A surface fit always requires a prechosen analytical form for the temperature dependence of the second (and third) virial coefficient. As for benzene [1], *n*-hexane [2], and *n*-octane [3], we applied

$$B(T)=\sum_{i=0}^{n}\frac{c_i}{T_R^i} \tag{16}$$

where

$$T_R=\frac{T}{T_c}=\frac{T}{540.15\ \mathrm{K}} \tag{17}$$

The SEEQ algorithm [12] was used to adjust the coefficients of Eq. (16). The derived second virial coefficients at nominal temperatures are presented in Table III and compared to results for other schemes detailed above. Two conclusions can be drawn from this table: First, the results from the two different surface fits differ by no more than 1% (no more than $7\ \mathrm{cm^3\cdot mol^{-1}}$). Second, the results according to scheme b differ from those determined from single isotherms (set 2) by no more than 2.3% (no more than $14.2\ \mathrm{cm^3\cdot mol^{-1}}$). These differences are within the assumed uncertainty of the second virial coefficients ($\pm 3\%$).

Nevertheless, it is worth stressing here that a surface fit of this kind always is a purely mathematical procedure and is to be used with caution. The raw $p\rho T$ data as well as the results of the surface fit need to be checked for a physically reasonable behavior. The latter would be possible for instance if scheme c could be applied and the derived temperature function $C(T)$ could be compared to results from model calculations or from corresponding-states approaches. The former was done by analysis of single isothermes as detailed above. Finally, analogous to our previous results [1–3], the second virial coefficients derived from the surface fit including correlated $C(T)$ [11] (set 4 in Table III) are considered to be the "true" values of this study and included in further analyses.

Table IV. Coefficients c_i in Eq. (16) (Final Correlation, B, in $cm^3 \cdot mol^{-1}$)

Coefficient			
c_0	c_1	c_2	c_3
1180.6248	−3559.7176	3166.5564	−1372.2934

4.4. Correlation of $B(T)$ Including Other Data

The results presented in Table III (set 4) have been included in a correlation for $B(T)$ together with selected data from the literature [13–16].

Based on a preliminary analysis, several data sets [17–23] from the literature were excluded from the correlation, because they show large deviations [22] from the entire body of data and/or a completely different temperature dependence compared with the preliminary fit [17, 20]. The results of Hirschfelder et al. [18], Zaalishvili [19], and Pompe and Spurling [23] are mainly based on the data of Smith et al. [17] and were not included in the primary data set. Finally, the data from Joule–Thompson measurements [21] were excluded from the primary data set because of the usually larger experimental uncertainty.

Table V. Correlated Second Virial Coefficients of *n*-Heptane

Temperature (K)	$B(T)$ ($cm^3 \cdot mol^{-1}$)
350	−1815.
375	−1478.
400	−1231.
425	−1046.
450	−903.1
475	−790.5
500	−699.5
525	−624.4
550	−561.1
575	−506.6
600	−458.9

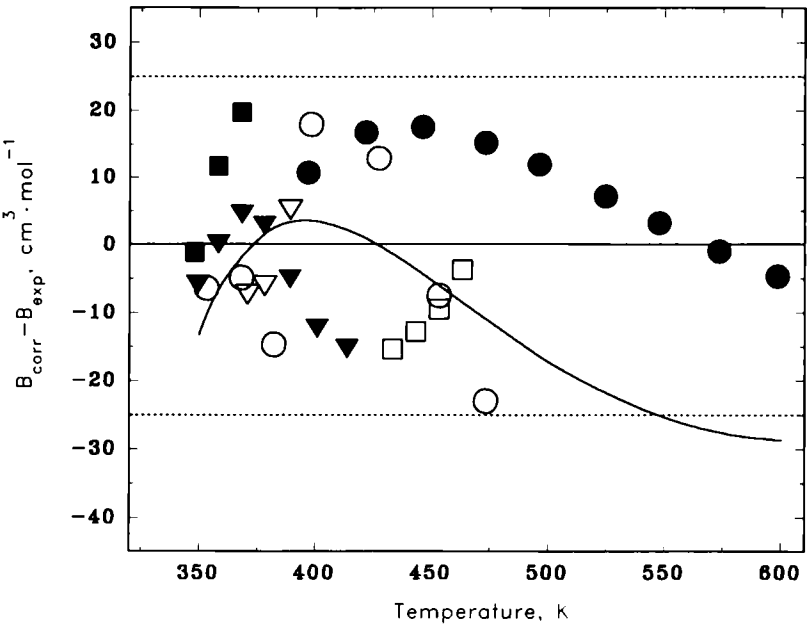

Fig. 5. Deviations of primary data from the final correlation. (▽) [13] Set 1; (▽) [13] set 2; (○) [14]; (□) [15]; (■) [16]; (●) this work; (——) [4] correlated.

Coefficients c_i have been determined using the analytical form of Eq. (16) together with Eq. (17). The results are summarized in Tables IV and V. The latter provides correlated values at selected temperatures to enable users to check their coding of the present correlation.

Accordingly, our correlation is based on data published by McGlashan and Potter (two sets) [13], Hajjar et al. [14] (data for $T \leqslant 0.65\ T_c$ not included because these were not corrected for higher virial coefficients), Belousova and Zaalishvili [15], and An Xueqin et al. [16] as well as on those presented here.

A comparison of the correlated data with the primary data set and the correlation of Dymond et al. [4] is shown in Figure 5. It becomes obvious from this plot that the maximum deviation associated to one experimental datum amounts to ±2.8% (no more than 30 $cm^3 \cdot mol^{-1}$), whereas the remaining data agree within 2%. The agreement with the correlation from Ref. 4 is excellent up to 450 K. At higher temperatures increasing differences are obvious, but these are well within ±30 $cm^3 \cdot mol^{-1}$.

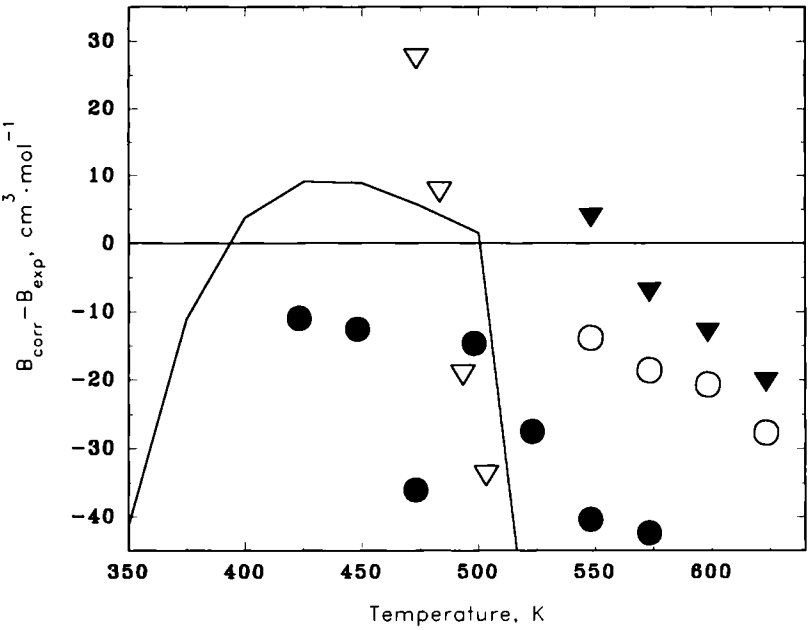

Fig. 6. Deviations of secondary data from the final correlation. (▽) [18]; (▽) [20]; (●) [22]; (○) [23]; (----) [21] correlated.

A comparison to secondary data is shown in Fig. 6. Generally, these data confirm the proposed correlation but show a larger scatter than it was found for the primary data. A completely different temperature dependence was derived by Al Bizreh and Wormald [21] for temperatures below 375 and above 500 K. It is obvious from the graph that this is not confirmed by the available experimental data.

5. CONCLUSIONS

Low-density $p\rho T$ data for *n*-heptane were measured in the temperature range 375–600 K. Above 473 K decomposition was found. Following correction for this small systematic error, the data were used to derive second virial coefficients. These have been included in the primary data set that was used to correlate $B(T)$ in the temperature range $320\,K \leqslant T \leqslant 600\,K$. The maximum uncertainty of the correlated data is assumed to be $\pm 3\%$ (maximum 25 $cm^3 \cdot mol^{-1}$).

APPENDIX

Table AI. $p\rho T$ Data Corrected for Nominal Temperatures and Decomposition (>473 K)[a]

Temperature (K)	Density ($mol \cdot m^{-3}$)	Pressure (kPa)
373.783	11.5424	35.2402
373.783	16.2492	49.2723
373.783	25.0146	74.8423
373.783	31.2406	92.5730
373.783	33.1477	97.9434
396.854	11.5419	37.5242
396.854	16.2486	52.5172
396.854	25.0136	79.9261
396.854	31.2394	99.0188
396.854	33.1464	104.820
396.854	38.5519	121.025
396.854	42.9464	133.922
396.854	47.8394	148.289
396.854	52.2144	160.773
421.645	11.5414	39.9454
421.645	16.2479	55.9732
421.645	25.0126	85.3244
421.645	31.2381	105.847
421.645	33.1450	112.085
421.645	38.5503	129.567
421.645	42.9447	143.513
421.645	47.8374	159.058
421.645	52.2122	172.626
446.120	11.5410	42.3460
446.120	16.2473	59.3528
446.120	25.0115	90.6230
446.120	31.2368	112.528
446.120	33.1437	119.184
446.120	38.5487	137.908
446.120	42.9429	152.848
446.120	47.8354	169.541
446.120	52.2101	184.143
473.166	11.5443	44.976
473.166	25.0189	96.438
473.166	31.2460	119.859
473.166	33.1534	126.969
473.166	38.5601	147.037
473.166	42.9555	163.052
473.166	47.8495	181.000
473.166	52.2255	196.694

[a] Each experimental datum presented in this table is the average of three independent readings.

Table AI. *(Continued)*

Temperature (K)	Density ($mol \cdot m^{-3}$)	Pressure (kPa)
496.125	11.5464	47.2203
496.125	16.2550	66.2629
496.125	25.0234	101.352
496.125	31.2517	126.044
496.125	33.1594	133.522
496.125	38.5671	154.721
496.125	42.9633	171.641
496.125	47.8582	190.629
496.125	52.2349	207.264
524.643	11.5453	49.9821
524.643	16.2534	70.1735
524.643	25.0210	107.442
524.643	31.2486	133.685
524.643	33.1562	141.658
524.643	38.5633	164.216
524.643	47.8535	202.515
524.643	52.2298	220.292
524.643	42.9591	182.281
547.642	11.5466	52.2127
547.642	16.2547	73.3329
547.642	25.0235	112.360
547.642	31.2516	139.838
547.642	33.1599	148.183
547.642	38.5674	171.847
547.642	42.9643	190.799
547.642	47.8586	212.071
547.642	52.2355	230.755
573.389	11.5470	54.7153
573.389	16.2558	76.8481
573.389	25.0247	117.839
573.389	31.2532	146.740
573.389	33.1611	155.516
573.389	38.5690	180.385
573.389	42.9655	200.368
573.389	47.8606	222.731
573.389	52.2375	242.435
598.398	11.5507	57.1495
598.398	16.2610	80.2995
598.398	25.0326	123.128
598.398	31.2632	153.398
598.398	33.1716	162.554
598.398	38.5813	188.646
598.398	42.9791	209.569
598.398	47.8758	233.012
598.398	52.2541	253.711

REFERENCES

1. E. Bich, H. Hendl, T. Lober, and J. Millat, *Fluid Phase Equil.* **76**:199 (1992).
2. E. Bich, T. Lober, and J. Millat, *Fluid Phase Equil.* **75**:149 (1992).
3. J. Millat, E. Bich, H. Hendl, and A. K. Neumann, *High Temp. High Press.*, in press.
4. J. H. Dymond, J. A. Cholinski, A. Szafranski, and D. Wyrzykowska-Stankiewicz, *Fluid Phase Equil.* **27**:1 (1986).
5. C. Tsonopoulos, J. H. Dymond, and A. Szafranski, *Pure Appl. Chem.* **61**:1387 (1989).
6. G. Opel and J. Schaffenger, *Wiss. Z. Univ. Rostock* **N18**:871 (1969).
7. J. Millat and G. Opel, *Wiss. Z. Univ. Rostock* **N38**:51 (1989).
8. T. Lober, Dissertation (Universität Rostock, Rostock, 1991).
9. E. Bich, M. Ramsdorf, and G. Opel, *Z. Phys. Chem. Leipzig* **265**:401 (1984).
10. H. Kammerlingh Onnes, *Comm. Phys. Lab. Leiden* No. 71 (1901).
11. H. Orbey and J. H. Vera, *AIChE J.* **29**:107 (1983).
12. K. M. de Reuck and B. A. Armstrong, *Cryogenics* **19**:505 (1979).
13. M. L. McGlashan and D. J. B. Potter, *Proc. Roy. Soc. (London)* **A267**:478 (1962).
14. R. F. Hajjar, W. B. Kay, and G. F. Leverett, *J. Chem. Eng. Data* **14**:377 (1969).
15. Z. S. Belousova and T. D. Sulimova, *Zh. Fiz. Khim.* **50**:981 (1976) (Russian).
16. An Xueqin, P. J. McElroy, R. Malhotra, Shen Weiguo, and A. G. Williamson, *J. Chem. Thermodyn.* **22**:487 (1990).
17. L. B. Smith, J. A. Beattie, and W. C. Kay, *J. Am. Chem. Soc.* **59**:1587 (1937).
18. J. O. Hirschfelder, F. T. McClure, and T. F. Weeks, *J. Chem. Phys.* **10**:201 (1942).
19. Sh. D. Zaalishvili, *Usp. Khim.* **24**:761 (1955) (Russian).
20. Z. S. Belousova and Sh. D. Zaalishvili, *Zh. Fiz. Khim.* **41**:1290 (1967) (Russian).
21. N. Al-Bizreh and C. J. Wormald, *J. Chem. Thermodyn.* **10**:231 (1978).
22. A. Zawisza and J. Vejrosta, *J. Chem. Thermodyn.* **14**:239 (1982).
23. A. Pompe and T. H. Spurling, *Virial Coefficients for Gaseous Hydrocarbons*, CSIRO Aust. Div. Appl. Org. Chem. Tech., Paper No. 1 (1974), p. 1.
24. C. P. Smyth and E. W. Engel, *J. Am. Chem. Soc.* **51**:2646 (1926).
25. S. Toscani, P. Figuiere, and H. Szwarc, *J. Chem. Thermodyn.* **21**:1263 (1989).
26. R. Malhotra and L. A. Woolf, *J. Chem. Thermodyn.* **23**:49 (1991).
27. J. A. Beattie and W. C. Kay, *J. Am. Soc.* **59**:1586 (1937).